**Benha Journal of Applied Sciences (BJAS)** **print: ISSN 2356–9751**
**Vol. (7) Issue (12) (2022), (85-107)** **online: ISSN 2356–976x**
**http://bjas.journals.ekb.eg**

# Textural analysis and environmental implications of the Late Pleistocene-Holocene sediments of the Faiyum paleolake, Egypt

**R.H. Badawy[1], M.A. Hamdan[2], Refaat.A. Osman[1], R.J. Flower[3], F.A. Hassan[4] and A.M. Afify[1]**
[1]Department of Geology, Benha University, Qalubia, Egypt
[2]Department of Geology, Cairo University, Cairo, Egypt
[3]Department of Geography, University College, London, UK
[4]Cultural Heritage Program, French University, Cairo, Egypt
E-mail:rounaq.badawy@fsc.bu.edu.eg

**ABSTRACT**

The Faiyum depression was linked to the Nile River and involved a broad freshwater lake, during most of the Holocene. Grain-size analysis of the lacustrine sediments along 22.7 m long core F3-08 of the Faiyum paleolake has been carried out to expose the mode of transportation, energy, and hydrodynamic conditions, as well as the environmental conditions. The recovered sedimentary sequence consists of predominantly siliciclastic lacustrine facies divided into six informal units. The grain size analysis of the studied sediments shows slight changes in the composition of the sediment mixture between silt and clay with rare occasional sand lenses. The variation in the standard deviation between well-sorted to poorly sorted sediments and from fine skewed to coarse skewed under leptokurtic to platykurtic nature exposes the environmental implications. Bivariate cross plots of grain size parameters, mode of transportation (C-M diagram), and linear discrimination functions (LDF) designate the fluvial nature of sediments and the riverine input. The depositional processes were aquatically controlled through active energy processes of the Nile flood. The graded suspension and suspension with rolling mode (saltation) are both the prime factors for transportation, where the sediments were deposited and reworked by turbidity actions, within a shallow agitated environment.

**Keywords:** Grain-size analysis, Lacustrine sediments, Geo-statistical parameters, Holocene, Faiyum, Egypt.

## 1. Introduction

Lakes are dynamic systems that integrate environmental, climatic and tectonic forcing into continuous high-resolution archives on local and regional scales (Gierlowski-Kordesch & Kelts, 2000). Grain size is a particularly valuable indicator of the hydrodynamic evolution of lakes because it corresponds to the hydraulic energy that is needed for clasts' transport, sorting, and deposition. The grain-size analysis provides paleoenvironmental information at a high temporal resolution. However, the typical polymodal grain-size distribution in lacustrine sediments has hindered the wide application of grain-size analysis as a standard tool. This polymodal grain-size distribution comes from different transporting media (e.g., floods, aeolian input, lake currents, and waves) and the re-sorting of sediment. However, within a lake, different depositional zones are characterized by distinctive combinations of grain size components. The textural analysis (grain size and shape) of lacustrine sediments has been used to reconstruct the changes in the hydrology of lakes corresponding to regional climatic and environmental conditions (Visher, 1969; Middleton, 1976; Ashley, 1978). Grain textural morphology is very important in understanding sedimentary processes like weathering, sorting and abrasion (Pettijohn et al. 1973).

Egypt deficits complete Holocene paleolimnological archives of environmental change (e.g. Hoelzmann et al., 2004). Lacustrine sediments often give natural archives of the Holocene paleoenvironmental changes. The Faiyum Depression, an Egyptian lake basin, can provide sedimentary records of Nile floods. (Flower et al., 2012; Hamdan et al., 2016; Marks et al., 2018). The sedimentary characteristics of lacustrine sediments reflect the actual nature of the lake and the inflow of water and are linked with the Nile. The early Holocene history of the Faiyum mega-lake (e.g. Hassan 1986, etc.) has been controlled by this river.

## 2. The geologic setting of the study area

The Faiyum province occupies a part of the northern Western Desert of Egypt to the west of the Nile Valley. It is located about 80 km southwest of Cairo covering a surface area of 12,000 km$^2$. It extends between latitudes 29°00′ and 30°00′ N and longitudes 30°15′ and 31°15′ E. Faiyum is unique in having access to water from a Nile branch (Bahr Yossef) through a narrow corridor, the Howara Channel (Hassan et al., 2012a). The irrigation of cultivatable land depended on this water coming from the Nile valley, instead of springs or deep wells like other oases. This branch delivered sediments freshwater through this passage into the Faiyum depression forming a wide freshwater lake (Little, 1936; Ball, 1939). The present study is based on a 22.7 m long drilled core (F3-08) of Holocene lacustrine sediments drilled in 2009 from the southern shore of modern Lake Qarun, 29°26’4.09’’ N, & 30°38’31.67’’ E (Fig. 1).

Freshwater diatomite deposits in the west and northeast areas of the Faiyum depression were found and an extensive freshwater lake (in historical sources, it is Lake Moeris) was detected during the Early Holocene (Wendorf and Schild, 1976). This lake level exceeded 20 m a.s.l. and it

was supplied by Nile water (Hassan and Hamdan, 2008). Since the Middle Holocene, Lake levels have reduced, and the vast ancient lake was a relatively small water body (Lake Qarun), following the climate and changes in Nile flood discharge. Now, it is confined to the northern and deepest part of the depression. The diminished modern Lake Qarun is 40 km long and up to 5.7 km wide; its surface is about 45 m below sea level and its mean and maximum depths fluctuate around 4.2 and 8.4 m, respectively. The lake is currently saline, and its salinity, in summer, is exceeding 30 $g^{-1}$. The saline water is mostly because of the great evaporation degree in the summer (Flower et al., 2006). The lake has gotten freshwater from the Nile via Bahr Yossef around 10 ka cal BP, since the early Holocene (Hassan, 1986; Flower et al., 2012). Freshwater amount from the annual Nile flood shrank during the second half of the last century, especially after the erection of the High Dam in 1961, and the lake suffered rising salinization.

The study aims are to show the distribution of grain size of the study area sediments and apply the relevant environmental implication of the grain size parameters to detect the depositional environment, interpret the energy and hydrodynamic conditions, and delineate the mode of transportation. Another aim is to observe in more detail the grain morphology and the light-mineral characteristics of the sand portion of the Faiyum area sediments along core F3-08.

## 3. Materials and methods

### 3.1. Sampling

The present study is based on a 22.7 m long drilled core (F3-08) of Holocene lacustrine sediments drilled in 2009 from the southern shore of Lake Qarun, 29°26'4.09'' N, & 30°38'31.67'' E by using a soil power-operated corer which allowed the recovery of enclosed sediment core sections (100 cm long and 9 cm wide). The encased Core F3-08 section was split longitudinally for examination and stratigraphic descriptions, lithological characteristics, color, grain morphology and sedimentary structures.

### 3.2. Sediment grain size analysis and heavy-light mineral separation

Particle size distribution of the F 3-08 core sediments was carried out using the wet sieving and hydrometer technique (Sawyer et al., 2008). Seventy-five samples at 30 cm intervals of core F 3-08 were selected to determine the distribution of clay (<2.5μm), silt (63-4μm), and sand (>63 μm). After removing carbonates by acid washing, the particle size distribution of sand-dominated contents was carried out using dry sieving techniques, and silt and clay fractions were determined using met methods. The >63 μm fraction was separated into light and heavy minerals with the use of bromoform liquid according to Milner (1962). In order to obtain the individual mineral percentage, coated and non-coated sediments, and also rounded and angular grains, the light grains were examined at x100 magnification under a binocular microscope to obtain their roundness by using the Powers (1953) photographic comparison charts, adapted to a logarithmic p scale (Folk, 1955). Mineral counting was performed by following the method of line counting of Galehouse, 1969, and the values were tabulated.

### 3.3. Petrographic studies

The texture and morphological characteristics were studied on 15 thin sections using an Olympus BX31 optical microscope.

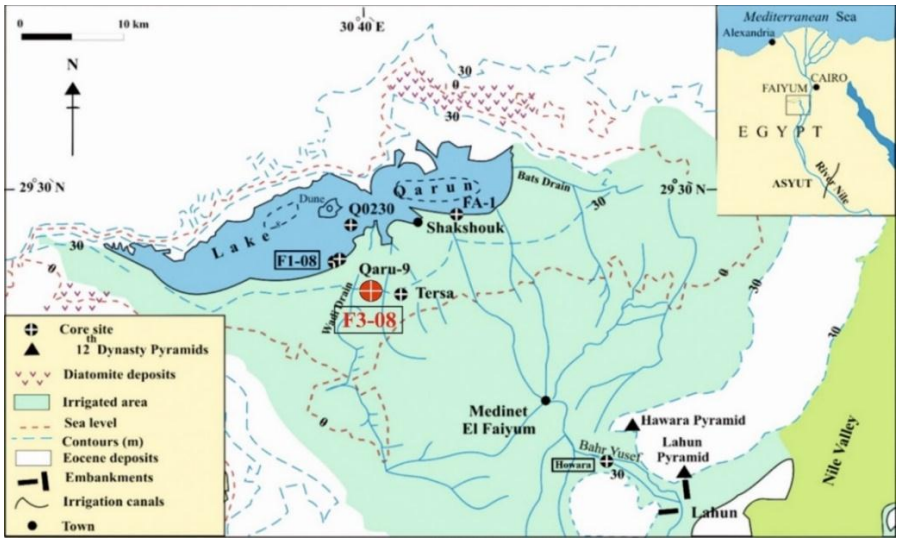


**Fig. (1)** Map of Faiyum depression showing the location of core F3-08 and other cores extracted in the area; Q0230 (Baioumy et al., 2010), Tersa (Hamdan et al., 2016), FA-1 (Marks et al., 2018), F1-08 (Hamdan et al., 2020a), and cores Qaru-9 (Hamdan et al., 2020b).

## 4. Results

### 4.1. Lithostratigraphy of the core sediments

Six sedimentary units have been defined in the studied core F3-08 according to their lithologies, color (using Munsell soil color charts), carbonate content, organic matter, bioturbation, magnetic susceptibility, and fossil content (Fig. 2) and summarized in Table 1.

**Table (1)** Summary of the six sedimentary units of core F3-08 (The chronology is established through cross-correlations based on sediment facies and magnetic susceptibility with well radiocarbon-dated cores i.e. core F1 (Marks et al., 2018) and core F1-08 (Hamdan et al., 2016; 2020; 2020b)).

| Unit | Chronology cal. ka BP | Depth (m) | Lithology | Fossil content | Sedimentary Environment |
|---|---|---|---|---|---|
| VI | 2-0 | 3-0 | Massive sandy clayey silt with abundant calcified root cast | Calcifies root casts | Floodplain environment |
| V | 4-2 | 4.7-3 | Massive sandy silty clay with abundant calcareous and rich in reworked pottery sherds as small fragments | Broken freshwater gastropods and rich in reworked pottery sherds as small fragments | Shallow lake environment |
| IV | 6-4 | 8.5-4.7 | Massive to faint laminated clayey silt with iron oxide laminae, few white carbonate laminae, and abundant carbonate and iron oxide concretions | Diatom and ostracods | Lacustrine delta front |
| III | 8-6 | 10.3-8.5 | Massive silty clayey with thin laminae (1-5 cm thick) of white carbonates laminae with less diatomite and floated clasts. | Diatom and ostracods | Lacustrine delta front |
| II | 10-8 | 16.6-10.3 | Interlaminated silty clay with very fine-grained quartzose sand | Diatom Ostracods and freshwater gastropods | Seasonal deep lake |
| I | >10 | 22.7-16.6 | The clay is inter-fingered with silty clay and overlain by coarse sand with well-rounded quartz grains. | Diatoms, rare freshwater gastropods and reworked Eocene foraminifera | Open deep lake And reworked bedrock Eocene clay |

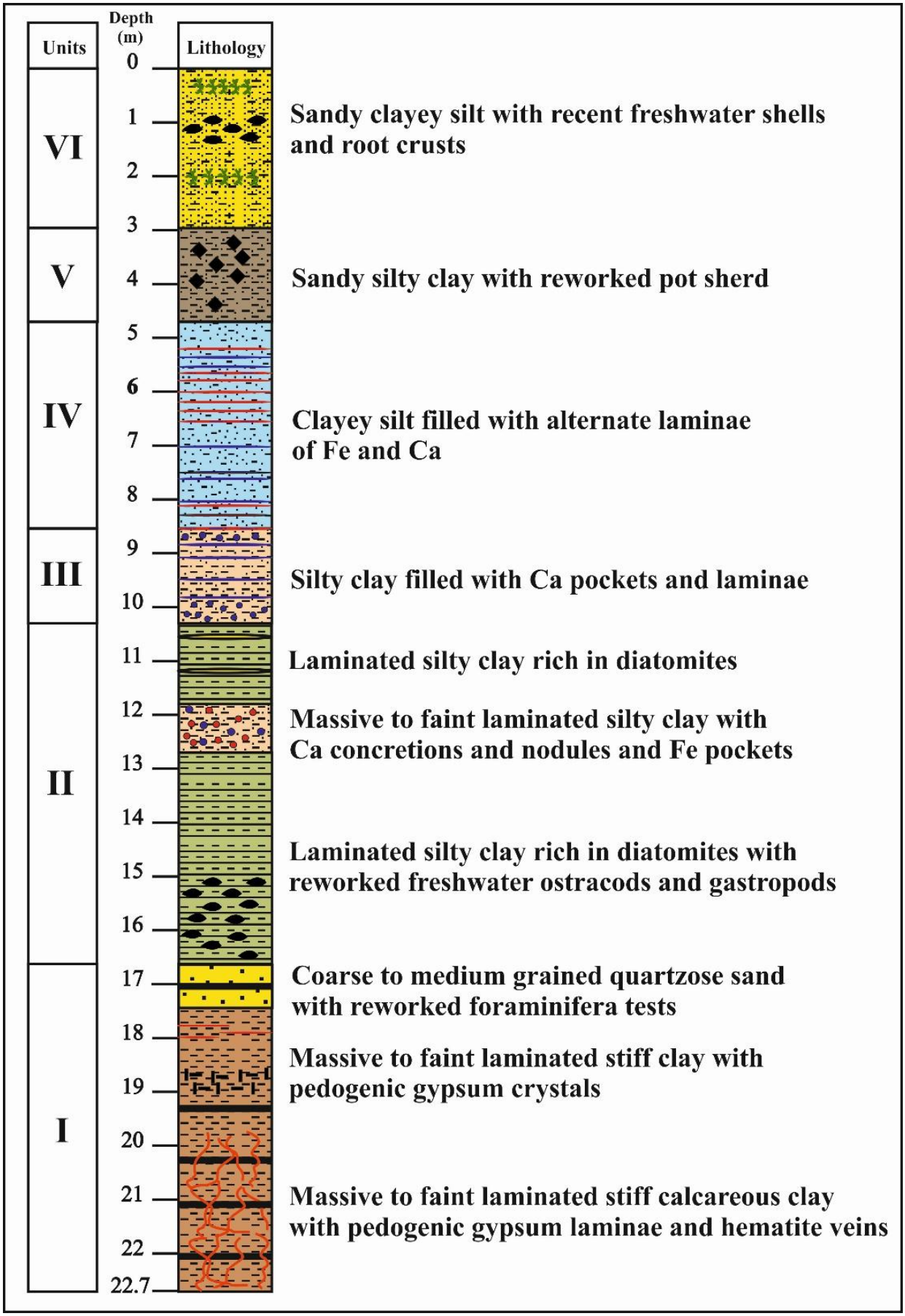


**Fig. (2)** Lithostratigraphy of core F3-08 sediments.

### 4.2. Grain size analysis

The results of the mechanical analysis are represented by histograms, cumulative diagrams, frequency curves, and distribution curves.

#### *4.2.1. Histograms*

The distributions of the different modes of the six units along the core are shown in Figure 3 where each sample in the figure represents the grain size histogram of the unit existent within it. The comparative study of the histograms of retained fractions of sieve analysis shows that most of these samples are of silt and clay, as most of the samples gave their highest column above class 0.0039 mm and <0.0039 mm, although some samples gave high percentages of sand in few places. The modes of 17 samples were of silt (Fig. 3A, C), two samples were of loamy sand (Fig. 3F), representing the interval at depth 19.17 m-19.79 m, and the modes of the 52 rest samples were of clay (Fig. 3B, D, E).

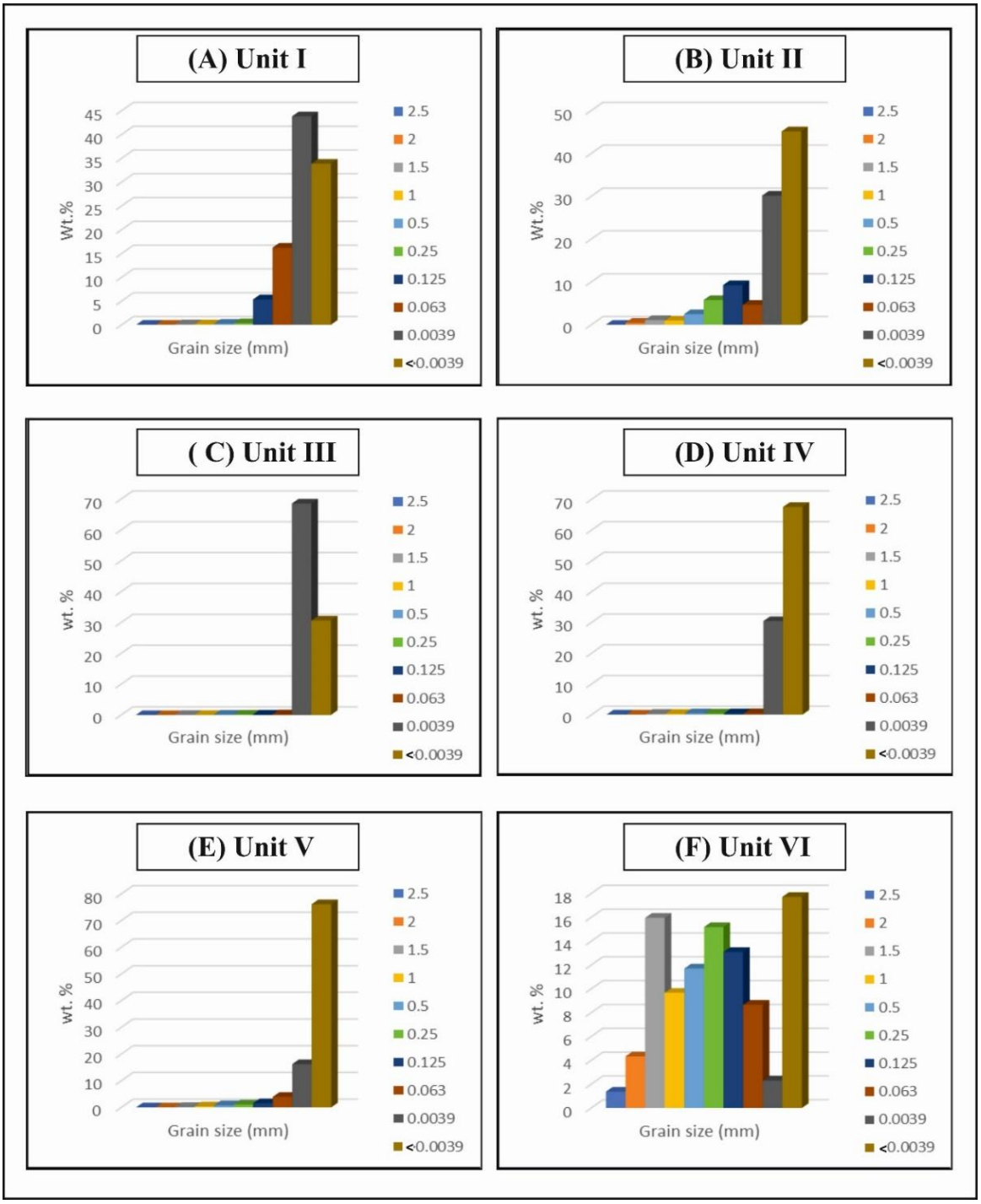


**Fig. (3)** Histograms of the six units of core F3-08.

### *4.2.2. Cumulative curves*

All the cumulative curves of the core (F3-08) consist of three segments representing three basic lithologies: sand, silt, and clay. This refers to different modes of transport. Most of these curves, except 13 ones, show no noticeable vertical change in grain size in the very fine-grained sand range, indicating a true suspension process of transport (Lane, 1938) (Fig. 4A, C, D, E). The 13 samples (1, 7, 8, 20, 23, 25, 27, 28, 30,117,140,143, and 145) with their different depths with medium to high percentages refer to the presence of graded suspension in the core (Fig. 4B, F). Towards the base of the bed, a graded suspension rises in grain size. The suspension method of transport makes most sedimentary laminae include some fine sand grains and smaller size fractions (Visher, 1969).

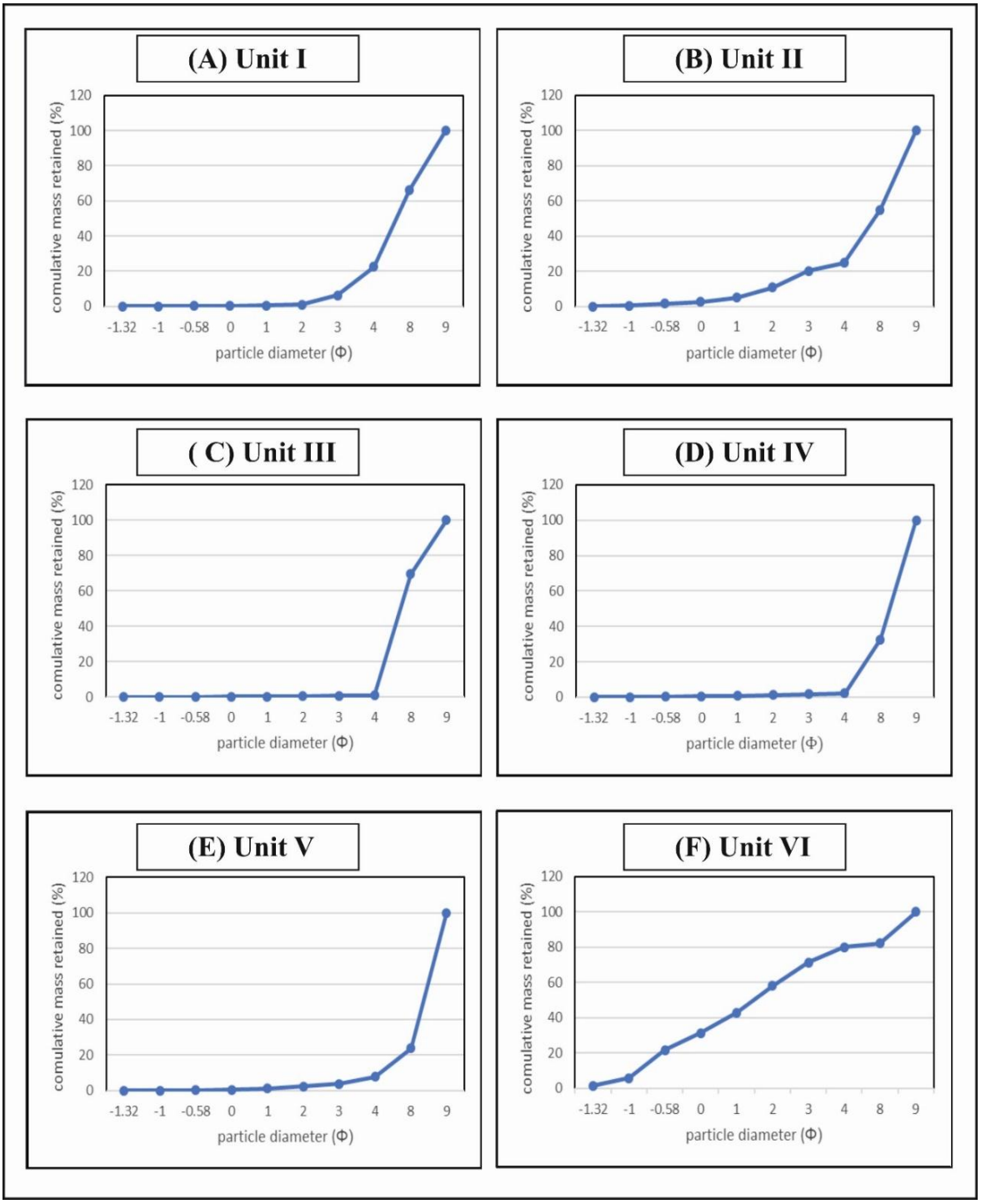


**Fig. (4)** Cumulative diagrams of the six units of core F3-08.

### *4.2.3. Frequency curves*

The frequency curves indicate that the grain sizes of the core (F3-08) are generally unimodal (Fig. 5A, C, D, E), except for 8 samples (1, 20, 23, 25, 27, 28, 30, and 117) which is bimodal (Fig. 5B) and 2 samples (140 and 143) are multimodal (Fig. 5F). They also show that most of the core is made of poorly to very poorly sorted sediment, as most of the frequency curves have wide range of shapes, except the last part of the core, 17.50m to 22.70m, which is moderate to well sorted (samples 127 to 168). All the frequency curves are negatively skewed, as they extend to the right part of the curve, representing silt, and clay. According to the normality, samples give 38 leptokurtic, 5 mesokurtic, and 32 platykurtic frequency curves at different depths along the core.

### *4.2.4. Distribution curves*

The distribution curves of core (F3-08) show the same trend and indicate that the core is generally made of a cycle of clay and silty clay with few places having high percentages of sand, This is produced in the presence of loamy sand, clay loam, and silty clay loam according to USDA. Each cycle of clay and silty clay ranges in thickness from 80cm to 4.1m in the biggest one. This is explained in Figs., 6 and 7.

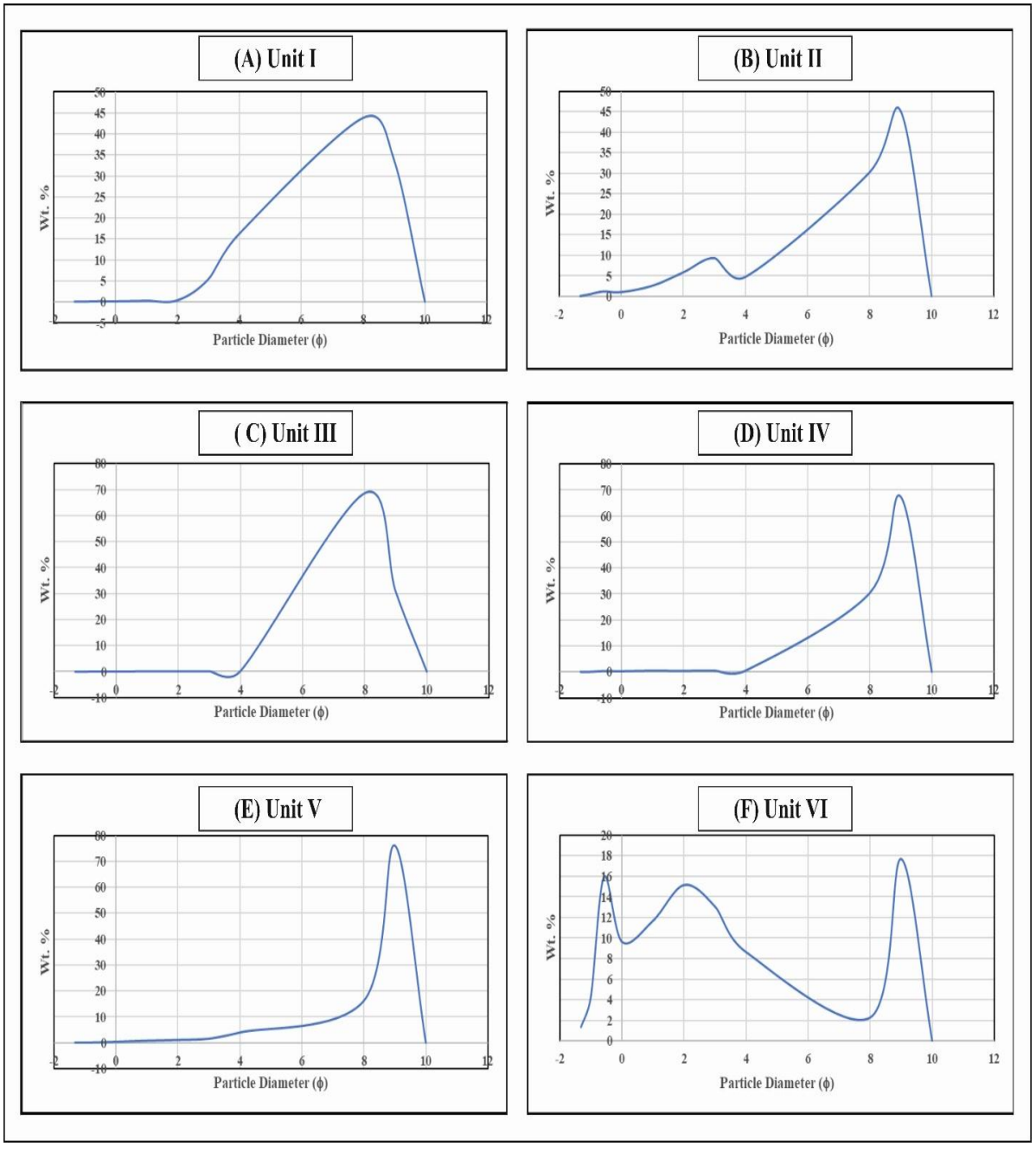


**Fig. (5)** Frequency curves of the six units of core F3-08.

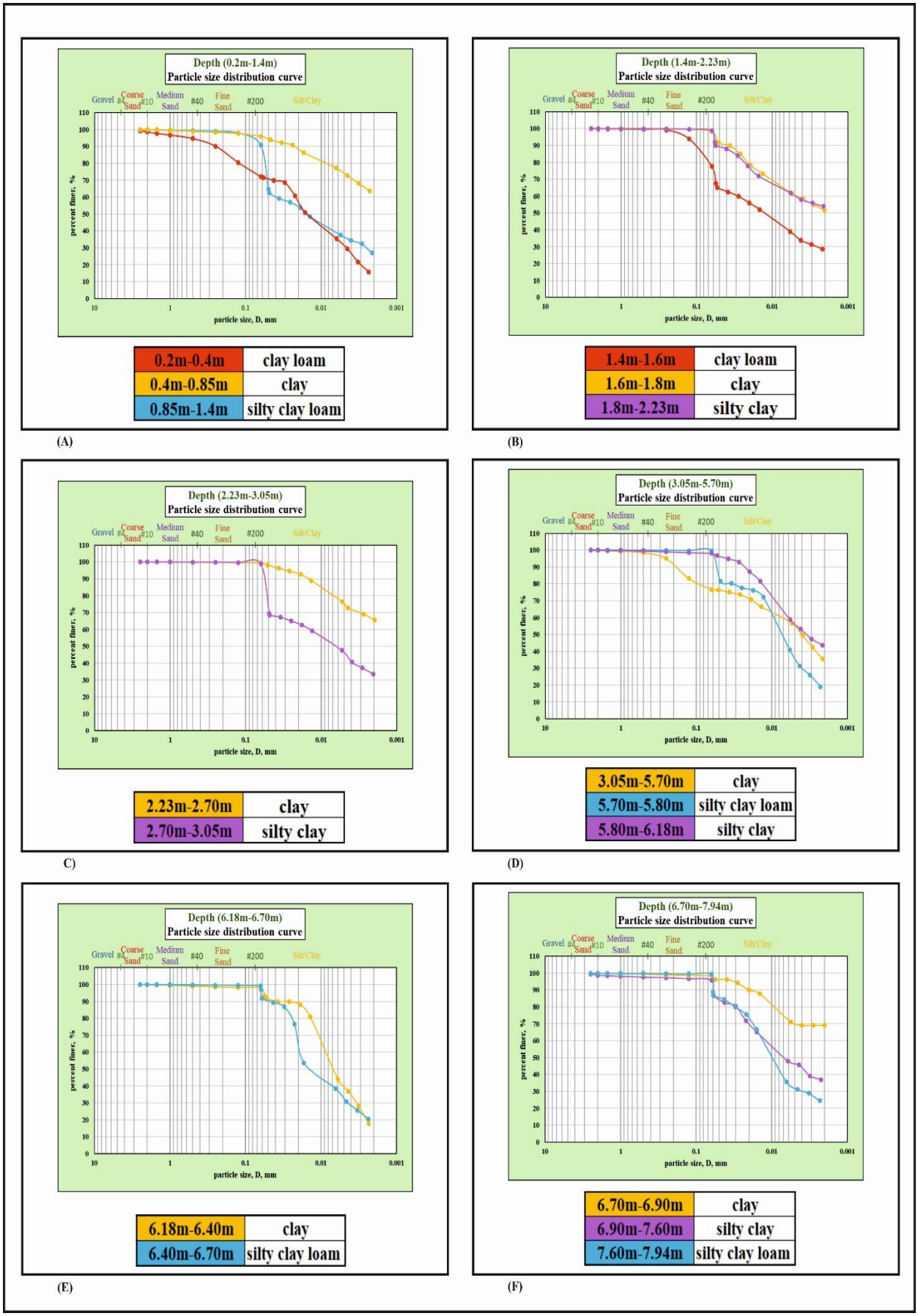


**Fig. (6)** Distribution curves of the six units of core F3-08.

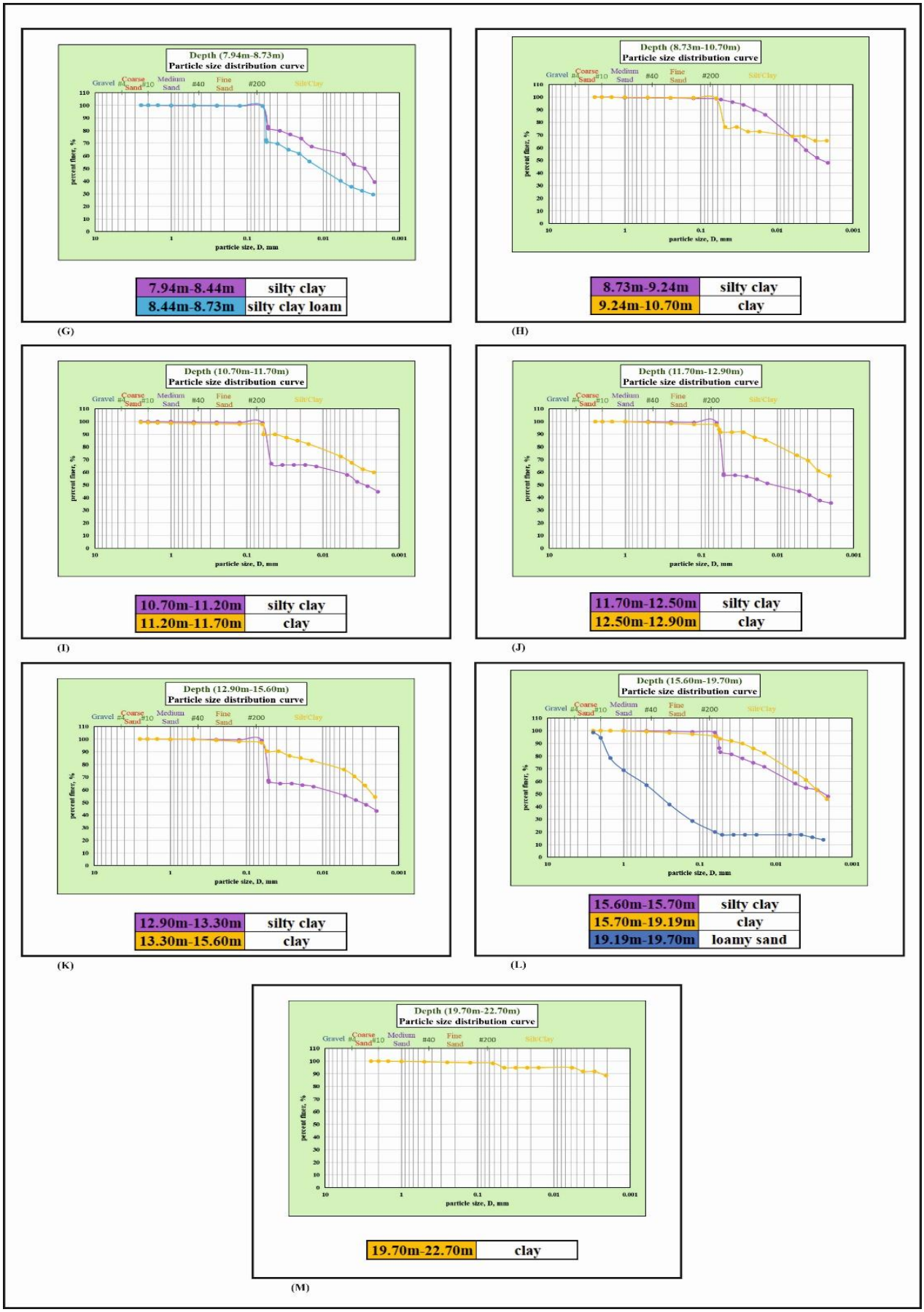


**Fig. (7)** Distribution curves of the six units of core F3-08.

### *4.2.5. Grain composition*

Grain size analysis of the core F3-08 (Fig. 8A) shows that the sediment is mainly clay (<4 µm) and subordinated with silt (4–63 µm). The basal part of the core, unit **I** (16.6-22.7 m), is approximately pure clay with >70% clay, but it has a channel of pebbly sand (80%) at 19.2 m-20 m. Unit II and Unit III (8.5-16.6 m) have high percentages of silt (50%) and high percentages of clay (70%), so they are silty clay. Unit IV shows the highest percentage of silt (>68%), it is clayey silt. In the upper part of the core (0-4.7 m), the average content of sand (> 63 µm) is relatively high at around 25%. Unit V (3-4.7 m) has a high content of clay, it is sandy silty clay. Unit VI (0-3 m) has a high content of silt, it is sandy clayey silt (Table 2).

### *4.2.6. Nomenclature and textural analysis*

The core texture analysis was made by defining the percentages of sand, silt, and clay in the samples. The classified fractions are plotted on the ternary plots (the soil texture analysis triangle of the United States Department of Agriculture (USDA Soil Texture ternary diagram; Fig. 9A and Folk ternary diagram 1974; Fig. 9B) for nomenclature of the sediments based on textural classification.

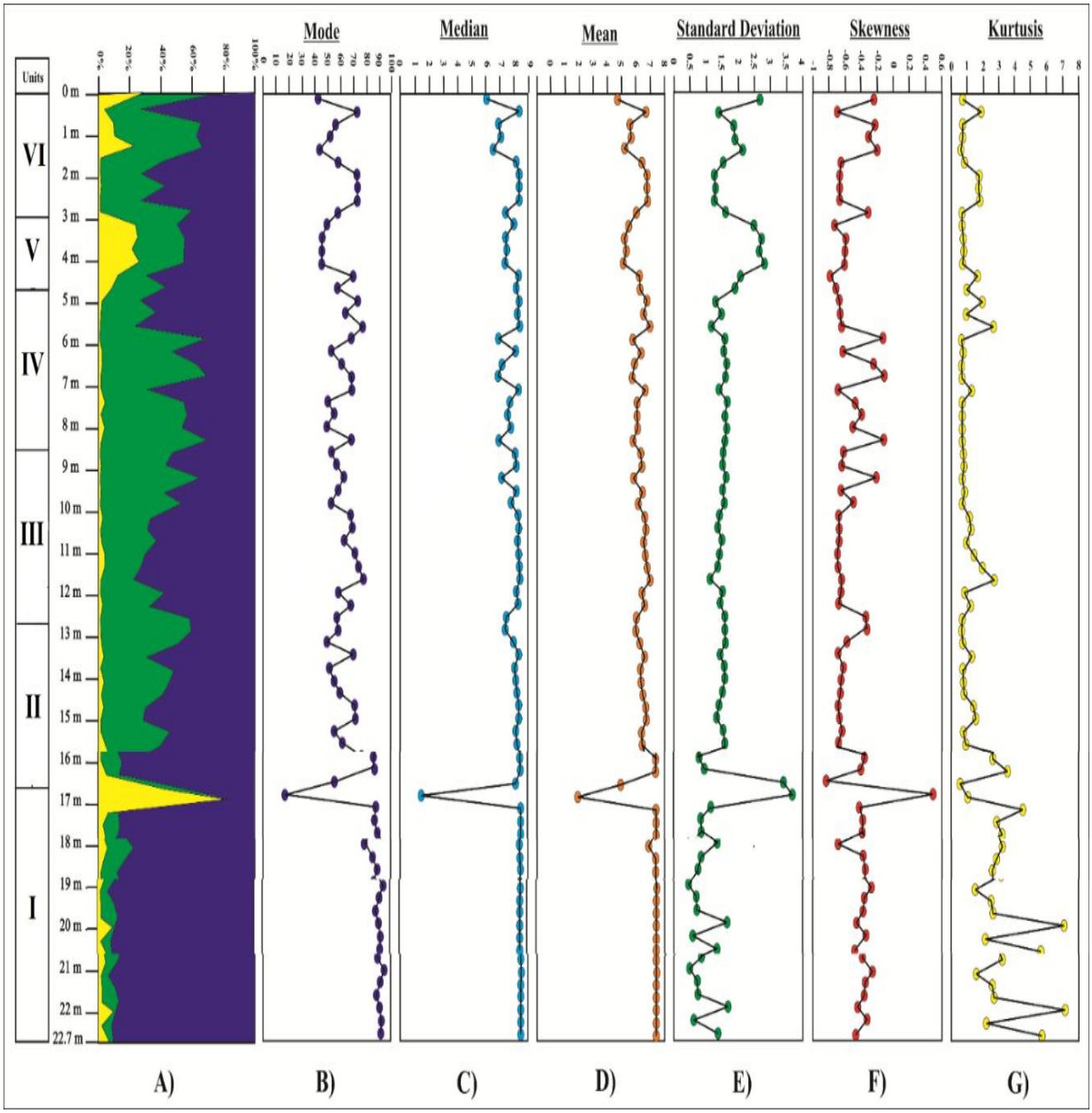


**Fig. (8)** Grain size composition and statistical parameters of core F3-08; (A) Grain size composition; (B) Mode; (C) Median; (D) Mean; (E) Standard deviation; (F) Skewness; (G) Kurtosis.

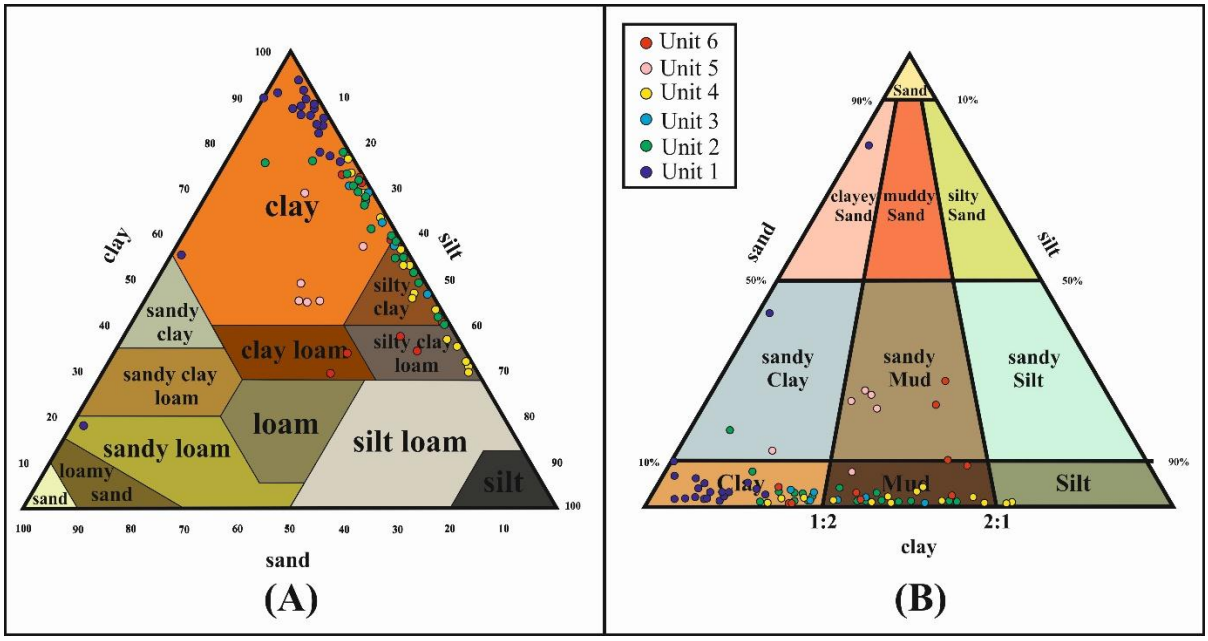


**Fig. (9)** Nomenclature of core F3-08 units through plotting samples on ternary diagrams (A) USDA Soil Texture ternary diagram, (B) sediment ternary diagram of Folk 1974.

### 4.3. Grain size statistical parameters

Grain size parameters were obtained by graphical and mathematical methods using the formulae proposed by Folk and Ward (1957). The values of ϕ5, ϕ16, ϕ25, ϕ50, ϕ75, ϕ84 and ϕ95 were obtained from the cumulative curves. The results are shown in Table 2 and discussed as follows.

#### *4.3.1. Mode (Mo)*

Mode values of core F3-08 range between 8ϕ and 9ϕ, indicating the dominance of silt and clay sediments (Fig. 8B). The basal part of the core (unit I) shows the mode of 9ϕ value representing clay. The middle part (units II and III) gives mode 8ϕ and most of the studied samples are with mode 9ϕ represented by silty clay. Unit IV shows 8ϕ mode (silt), with a few 9ϕ mode (clay) forming clayey silt. Unit V is the clay of 9ϕ mode, with only one sample of 8ϕ mode. Unit VI has a mixed mode like unit IV forming clayey silt.

#### *4.3.2. Median (Md)*

Median values of core F3-08 (Fig. 8C) are ranging between 6ϕ and 8.3ϕ. 6ϕ and 7ϕ values are corresponding to the silt sediments, but values equal to 8ϕ or more are of clay. Unit I shows values of more than 8ϕ of clay, with only one low value of 1.5 corresponding to the sand channel. The middle part (units II and III) gives 8.36-7.37, silty clay. Unit IV shows 8.35-6.87ϕ, with more silt. Unit V shows 8.28-7.36ϕ, with more clay. Unit VI has 8.31-6.07ϕ with more silt percentages like unit IV.

#### *4.3.3. Graphic Mean size ($M_Z$)*

Mean size values of core F 3-08 (Fig. 8D) are ranging between 2.94ϕ and 8.46ϕ with an average of 5.7ϕ. Unit I shows values from 8.47ϕ fall in the clay grade to 2.94ϕ fall in the medium sand grade. Unit II ranges from 7.99ϕ to 6.9ϕ fall in the clay and silt grades. Unit III ranges from 7.68ϕ to 7.2ϕ fall in the clay and silt grades. Unit IV ranges between 7.95ϕ and 6.75ϕ fall in the clay and silt grades, with more silt. Unit V ranges between 7.29ϕ and 6.13ϕ fall in the clay and silt grades, with more clay. Unit VI ranges between 7.8ϕ and 5.69ϕ fall in the clay and silt grades, with more silt percentages like unit IV.

#### *4.3.4. Inclusive graphic standard deviation ($\sigma_I$)*

Sorting coefficient values of core F3-08 (Fig. 8E) range between 3.68 (very poorly sorted) and 0.49 (well sorted) with an average of 2.085 (very poorly sorted). Unit I ranges from 3.69 (very poorly sorted) to 0.49 (well sorted), but most of the samples in this unit are moderately sorted. Unit II ranges from 2.73 (very poorly sorted) to 1.13 (poorly sorted). Unit III ranges from 1.56 to 1.36 of poorly sorted sediments. Unit IV ranges from 1.66 to 1.15 of poorly sorted sediments. Unit V ranges from 2.8 (very poorly sorted) to 1.89 (poorly sorted). Unit VI ranges between 2.65 (very poorly sorted) and 1.26 (poorly sorted).

#### *4.3.5. Inclusive graphic skewness ($SK_I$)*

Inclusive graphic skewness values of core F 3-08 range between 0.49 (very fine skewed) and -0.85 (very coarse skewed) with an average of -0.18 (coarse skewed) (Fig. 8F). Unit I ranges from 0.5 (very fine skewed) to -0.84 (very coarse). Unit II

ranges from -0.32 to -0.85 (very coarse skewed). Unit III ranges from -0.49 to -0.69 (very coarse skewed). Unit IV ranges between -0.12 (coarse skewed) and -0.68 (very coarse skewed). Unit V ranges between -0.59 and -0.79 (very coarse skewed). Unit VI ranges between -0.21 (coarse skewed) and -0.69 (very coarse skewed). Negative values of skewness indicate high concentrations of silt and clay.

#### *4.3.6. Graphic kurtosis ($k_G$)*

Graphic kurtosis values of core F3-08 (Fig. 8G) range between 0.6 (very platykurtic) and 7.15 (extremely leptokurtic) with an average of 3.88 (Extremely leptokurtic). Unit I ranges from 7.15 (extremely leptokurtic) to 0.6 (very platykurtic). Unit II ranges from 5.84 (extremely leptokurtic) to 0.69 (platykurtic). Unit III ranges from 1.44 (leptokurtic) to 0.72 (platykurtic). Unit IV ranges between 1.9 (very leptokurtic) and 0.68 (platykurtic). Unit V ranges between 1.63 (very leptokurtic) and 0.67 (very platykurtic). Unit VI ranges between 1.86 (very leptokurtic) and 0.62 (very platykurtic).

### 4.4. Petrography of sand fraction

In the present study, the distribution and morphological properties of detrital grains have been studied. The grain morphology of the studied core samples is represented by grain roundness and coating.

#### *4.4.1. Distribution of light minerals*

The distribution percentages of the light minerals of core F3-08 are represented in Fig. 10A and Table 3 in their arithmetic average values according to each unit indicating that they are variable throughout the core. Unit I has moderate values (0.1 to 6.5%), but at a depth of 19.5m, there is an extremely high peak (28.7%) of light mineral. Units II**,** III, and IV have low to moderate values (0.09 to 4.7%), with another peak (20.7%) at a depth of 16.2m. The highest values of the percentages of light mineral distribution belong to units V and VI (0.24 to 20.5%).

There are several sources of the detrital sands; among that Nile sources, local sources washed from Oligocene sandstone and Eocene limestone by local streams, and finely wind-blown sand. The light minerals of the sediments of core F3-08 consist of three main mineral groups; quartz, feldspar, and rock fragments. Quartz grains consist of monocrystalline and polycrystalline types (Fig. 11A) and could be derived from any of the above-mentioned sources. Nile sands are rich in mono- and polycrystalline quartz, however, the sand transported from Ethiopia contains a high percentage of polycrystalline than those transported from central Africa (Garzanti and Andò, 2015). Quartz grains that are transported from Oligocene sand contain a high percentage of undulated monocrystalline quartz. Feldspar grains are represented by plagioclase (Fig. 11B) and K. feldspar (microcline) (Fig. 11C). Feldspar grains of the sediments of core F3-08; could refer to their sources, where K. feldspar is transported from central African sources and abundant plagioclase grains are from Ethiopian sources. Rock fragments are represented mainly by volcanic igneous rock and limestone sands. The igneous rock fragments have two sources; these are local Oligocene basalts (north of the lake) and Nile sources derived from Ethiopian highlands. The difference between these two sources could be indicated based on the degree of alteration where the Nile basalt rock fragments are much more altered than local ones. Carbonate fragments are the second most abundant group of light minerals in core F3-08 sediments (Fig. 11D).

**Table (2)** Average statistical parameters of the six units of core F 3-08.

| Unit | Depth (m) | Grain size composition | | | Statistical parameters | | | | | | | |
|---|---|---|---|---|---|---|---|---|---|---|---|---|
| | | Sand % | Silt% | Clay% | Mode | Mean | Median | Standard Deviation | | Skewness | | Kurtosis |
| **VI** | 0m-3m | 7.89 | 41.08 | 51.03 | 8.83 | 7.9 | 7.95 | 1.25 | Poorly sorted | -0.35 | Very coarse skewed | 3.05 | Extremely leptokurtic |
| **V** | 3m-4.7m | 19.24 | 28.67 | 52.09 | 8.83 | 7.9 | 7.97 | 1.26 | Poorly sorted | -0.37 | Very coarse skewed | 3.07 | Extremely leptokurtic |
| **IV** | 4.7m-8.5m | 1.47 | 48.71 | 49.82 | 8.83 | 7.93 | 8 | 1.23 | Poorly sorted | -0.37 | Very coarse skewed | 3.06 | Extremely leptokurtic |
| **III** | 8.5m-10.3m | 1.63 | 35.88 | 62.49 | 8.83 | 7.92 | 8.01 | 1.24 | Poorly sorted | -0.39 | Very coarse skewed | 2.97 | Very leptokurtic |
| **II** | 10.3m-16.6m | 3 | 34.72 | 62.29 | 8.83 | 7.92 | 8.03 | 1.25 | Poorly sorted | -0.4 | Very coarse skewed | 2.97 | Very leptokurtic |
| **I** | 16.6m-22.7m | 9.35 | 9.63 | 81.02 | 9 | 7.91 | 8.05 | 1.25 | Poorly sorted | -0.42 | Very coarse skewed | 2.96 | Very leptokurtic |

### *4.4.2. Roundness*

Roundness describes the degree of abrasion of clastic fragments and provides evidence of time and distance of transport in different sedimentary environments (Kasper-Zubillaga et al., 2005). The core sands are characterized by a distribution pattern of roundness with a modal class that varies from angular to rounded concerning the size fractions. The percentages of every type are present in Table 3 in their arithmetic average values according to each unit. The roundness classes of both fine and medium sand fractions of core F 3-08, using a 30cm interval are shown in Fig. 10B. This study confirms that increasing roundness is associated with an increase in grain size. Angular classes predominate in the fine-size fraction, and the rounded classes are dominated in the medium sand fraction.

The roundness of unit I is much better than the other units but has relatively high values of sub-rounded and sub-angular. Sub-unit (b) of unit II has the highest percentage of rounded grains (32%) (Fig. 17-B). Unit III has high values of rounded and sub-rounded grains. The poorest roundness of core F3-08 clasts is recorded in units IV and V . Unit VI has moderate values of rounded sediments and also of angular sediments, but relatively high values of sub-rounded and sub-angular ones.

### *4.4.3. Coating*

The coating is a measure of the transporting agent to identify the depositional environment. In the studied core, the coated, sub-coated, and non-coated grains were counted from the thin sections. The percentages of every type are shown in Table 3 in their arithmetic average values according to each unit and plotted in Fig. 10C. The curve of coating shows that the grains vary from coated to non-coated along the core (Fig. 10C). Coated sediments are present with moderate to high percent along the core. The curve shows the highest order of coated sediment values in units III and IV (72-92.6%). Unit VI has the highest value of non-coated sediments at 68%. Non-coated sediments are also high at the sandy channel of unit I, unit II, and unit V.

**Table (3)** Average values of roundness and coating of the six units of core F 3-08.

| Unit number | Depth (m) | L. M. Wt.% | Roundness | | | | Coating | | |
|---|---|---|---|---|---|---|---|---|---|
| | | | Angular % | Sub angular % | Sub rounded % | Rounded % | Coated % | Sub Coated % | Non-Coated % |
| **VI** | 0m-3m | 7.69 | 14.52 | 41.03 | 35.16 | 9.29 | 29.47 | 31.46 | 39.07 |
| **V** | 3m-4.7m | 8.95 | 19.68 | 44.57 | 30 | 5.75 | 26.36 | 41.65 | 31.99 |
| **IV** | 4.7m-8.5m | 0.74 | 23.96 | 42.57 | 23.62 | 9.86 | 61.07 | 25.87 | 13.06 |
| **III** | 8.5m-10.3m | 2.28 | 20.22 | 36.84 | 28.55 | 14.39 | 58.58 | 21.27 | 20.16 |
| **II** | 10.3m-16.6m | 2.29 | 18.83 | 33.37 | 30.8 | 16.99 | 42.21 | 35.11 | 22.68 |
| **I** | 16.6m-22.7m | 5.99 | 19.08 | 32.79 | 31.21 | 16.92 | 32.9 | 33.46 | 33.64 |

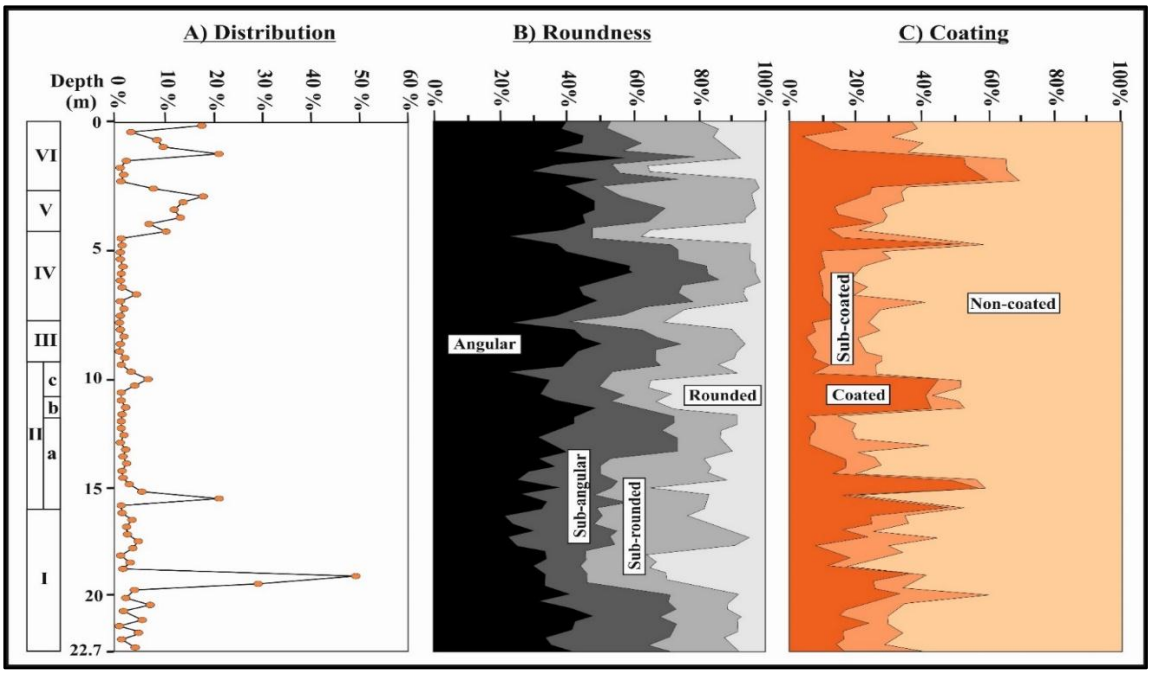


**Fig. (10)** Distribution of detrital light minerals, roundness, and coating down the core F3-08.

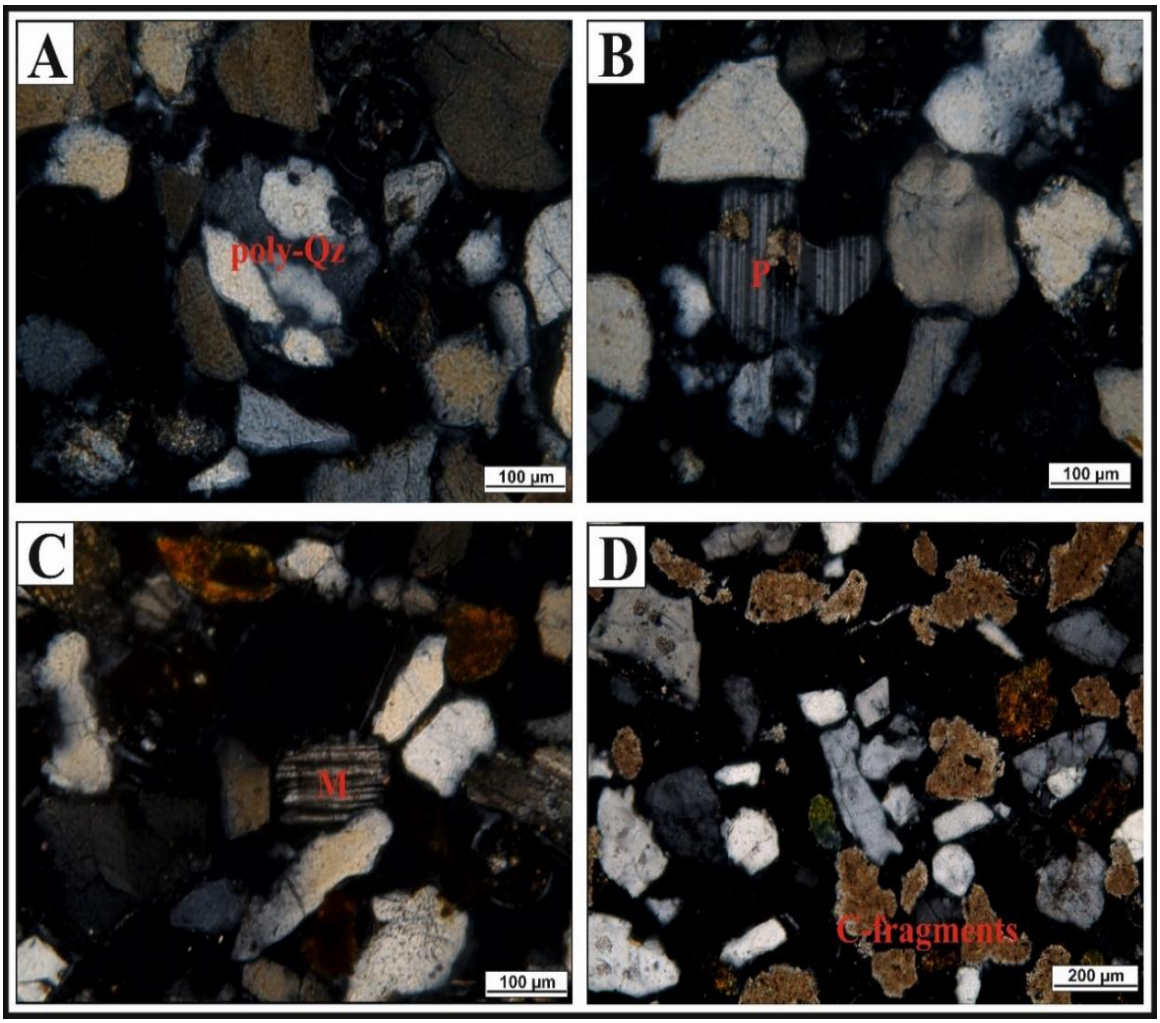


**Fig. (11)** Light sediments of core F3-08: (A) Polycrystalline quartz, (B) Plagioclase, (C) Microcline, (D) Carbonate rock fragment.

## 5. Discussion

### 5.1. Implications of grain size parameters

Silt is the dominant size observed in the investigated samples of core (F 3-08), signifying a narrow range of sediment size and indicating a consistent depositional environment. The distribution curves of the six units display a predominant silt population mixed with varying subordinate populations (mainly clay; and very fine sand subpopulations). The dominance of fine grains is attributed to the Nile source nature of the sediment. There is obvious discrimination in the textural characteristics of the late Pleistocene and Holocene lacustrine sediments of core F3-08. The former has a mean size ($M_Z$) dominated by very fine silt to clay and fine-grained sand size at contact with the overlying unit II. The dominant and homogeneous distribution of clay size along with unit I probably indicates the stable depositional condition of a large and deep lake. The Holocene lacustrine sediments (units II-V) are represented by fine sand to fine silt. The early Holocene sediments (unit II) show a range of grain size between fine to very fine silt, while the early middle sediment (unit III) shows a very narrow range of fine silt size. The late middle and late Holocene sediments (units IV & V) are characterized by a coarsening trend from fine to coarse silt sizes (Fig. 12A). Unit VI show a wide range of mean size from medium to very fine silt. Generally, the calculated mean values for the six units point to the gradual increase in mean values towards the top of the core.

The inclusive graphic standard deviation values fluctuate between moderately poorly-sorted to very poorly-sorted sediments throughout the six units of the core suggesting a low-energy environment. The moderately well-sorted nature increases towards the bottom of the core, at unit I, which resulted from the intermixing of different fractions of sediments in varying proportions. The moderately well-sorted nature is attributed to the addition of coarse fractions and removal of fines when the lake dries up through the reworking and the aeolian processes (Fig. 12B).

Skewness ($Sk_I$) values along the six units vary from very coarse-skewed to very fine-skewed fields, indicating the prevalence of a mixed energy environment. The skewness ranges values according to units are represented in Fig. 12C. The coarsening up of the sediments corresponding to the continuous lowering of lake level throughout the Holocene is supported by the prevailing negative skewness of units III, IV, V & VI. Negative skewness reflects the abundance of the coarse-grained tail in the whole sediment that proposed a high energy condition. The positive skewness nature that dominated unit II and a big range from unit I reflects that these parts are dominated by relatively low energy conditions resulting in the accumulation of finer sediments in a deep lake (Fig. 12C).

The disparity in the kurtosis values signs of the flow characteristic of the depositional environment (Ray et al., 2006). The extremely leptokurtic to platykurtic nature indicated multiple environments processing prevailing along the core and the energy fluctuations of the depositional medium. Kurtosis range values are represented in Fig. 12D. The dominance of extremely leptokurtic nature in units I and II is due to the maximal energy action and the mesokurtic nature could be related to the minimal action of high energy factor resulting in continuous supply (stream) of finer sediment materials in variable amounts.

### 5.2. Depositional environment (Grain size bi-variant relations)

Bi-variant relations of statistical grain size parameters are significant in identifying mechanisms of sediment transportation and differentiate the depositional environments, as the textural parameters of the sediment are often environmentally sensitive (Folk and Ward, 1957; Passega, 1957; Friedman, 1967; Moiola and Weiser, 1968; Visher, 1969; Sutherland and Lee, 1994).

#### *5.2.1. Mean size versus standard deviation*

The mean size *vs.* standard deviation plot of the present samples (Fig. 13A) shows the nature of the sediments is dominantly bimodal, of which, the dominant constituent is silt. The clay is subordinate which makes the admixture a poorly sorted nature. The relation shows that the sediments of units II-VI of core F3-08 are in the zone of silt size and range from poorly sorted to very poorly sorted. Unit I is clay and ranges from moderately sorted to well sorted, with only one sample of loamy sand and very poorly sorted.

#### *5.2.2. Mean size versus skewness*

The mean size *vs.* skewness (Fig. 13B) indicates the nature of sediments with a higher percentage of silt and subordinate clay. The skewness classification indicates coarse sediments and is predominantly negative. This is due to the mixture of two sizes of classes of sediments. This blending gives negative or positive values of skewness reliant on the ratios of size classes in the mixture. The present values are mostly falling in the negatively skewed zone of the graph; however, a few samples are positively skewed. The graph indicates that the sediments of all the units of core F3-08 are in the zone of silt size, except unit I of clay. All the sediments range from coarse skewed to very coarse skewed. Only one sample of unit I is fine sand and very fine skewed.

#### *5.2.3. Mean size versus kurtosis*

The relation between mean size and kurtosis (Fig. 13C) shows the blending of two size classes of sediments, that affect the graph in tails and peaks. The diagram shows that the sediments of units II-VI of core F3-08 are in the zone of silt size and range from very platykurtic to platykurtic. Unit I is clay and ranges from extremely leptokurtic to leptokurtic.

### *5.2.4. Skewness versus standard deviation*

The graph of skewness vs. standard deviation (Fig. 13D) reveals that all the sediments of core F3-08 are coarse to very coarse skewed. Sorting is different along the core. Unit I ranges from well-sorted to poorly sorted. Units II, III, and IV are poorly sorted. Units V and VI are very poorly sorted.

### *5.2.5. Skewness versus kurtosis*

The plot of skewness *vs.* kurtosis interprets the genesis of sediment, depending on the degree of normality of its size distribution (Folk, 1966). The plot indicates that coarse skewed sediments are platykurtic (Fig. 13E). Sediments of very coarse skewed range from platykurtic to extremely leptokurtic according to their units (Fig. 13E). Unit I is very extremely leptokurtic and Units II and III are mesokurtic. Unit IV and unit V are platykurtic and Unit VI is platykurtic to very leptokurtic.

### *5.2.6. Standard deviation versus kurtosis*

The plot between standard deviation and kurtosis (Fig. 13F), shows that most of the sediments, units II-VI, are poorly sorted to very poorly sorted with kurtosis from platykurtic to leptokurtic. Unit I is well sorted to poorly sorted with kurtosis ranging from very leptokurtic to extremely leptokurtic.

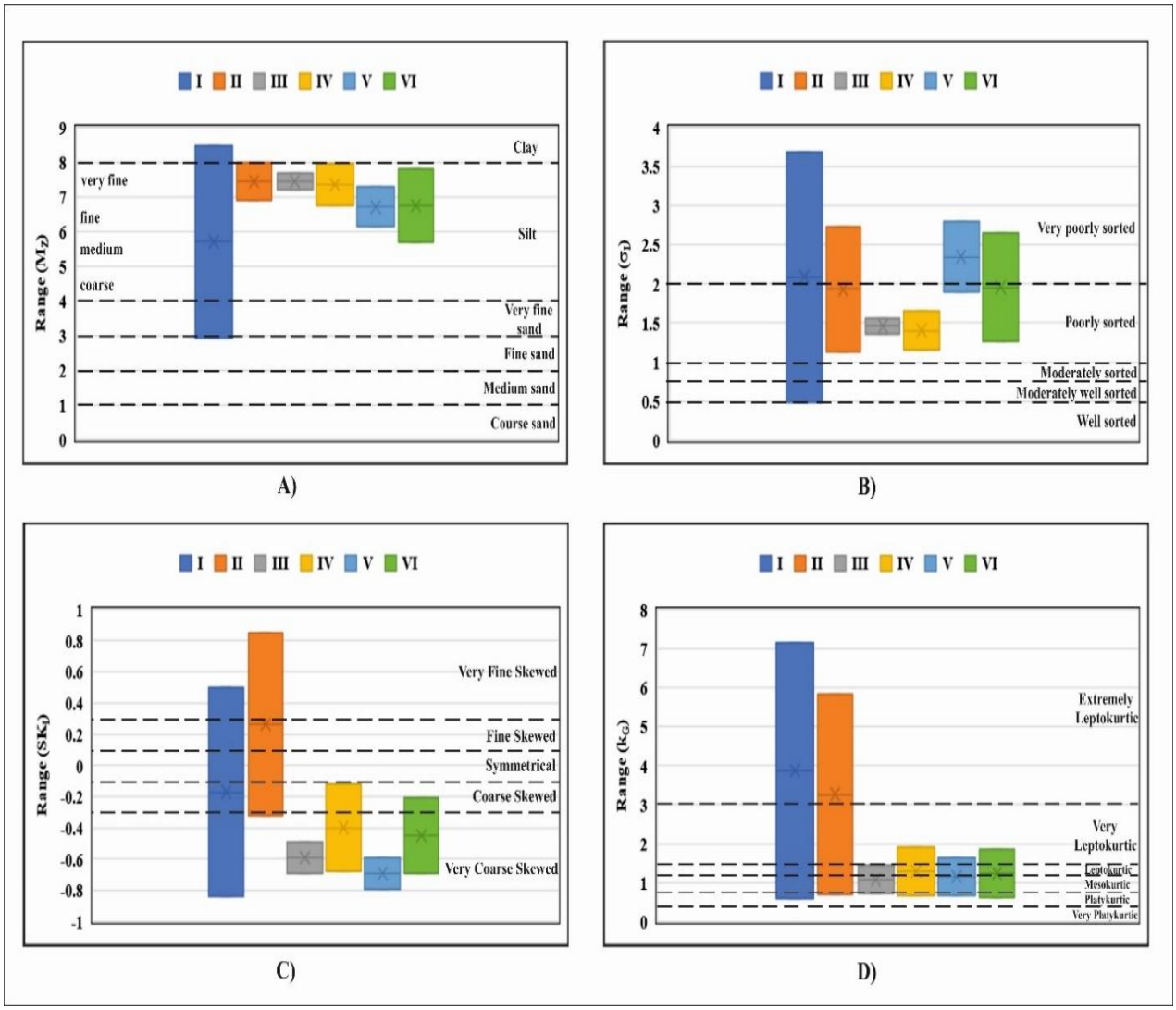


**Fig. (12)** Range box plots of (A) mean size ($M_z$); (B) standard deviation ($\sigma_I$); (C) skewness ($Sk_I$); (D) kurtosis ($K_G$) of core F3-08 units.

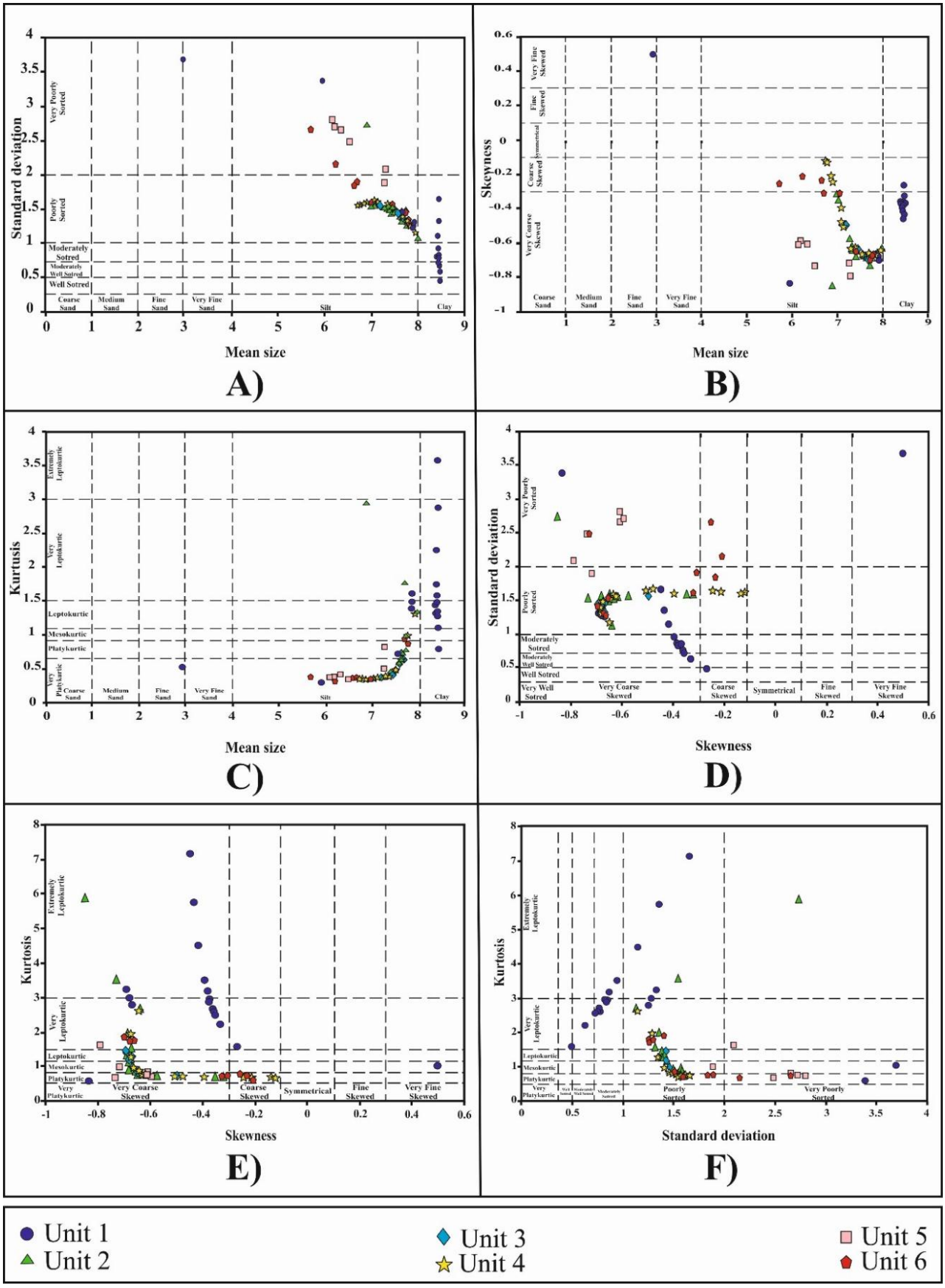


**Fig. (13)** Core F3-08 bivariate cross plots between (A) Mean size and standard deviation; (B) Mean size and skewness; (C) Mean size and kurtosis; (D) Skewness and standard deviation; (E) skewness and kurtosis; (F) Standard deviation and kurtosis.

### 5.3. Energy and Hydrodynamic Conditions (Cross-correlation of LDF (Linear discriminate function))

The Linear discrimination function (LDF) is a statistical analysis of the sediments used to interpret the fluidity factor and energy variations and compare the different processes of the depositional environment (Sahu, 1964). Four equations for four discriminant functions (Y1, Y2, Y3, and Y4) to distinguish between the sedimentary environments were stated by Sahu (1964). The discriminant functions have been calculated in dependence on the mean size (Mz), standard deviation $(\sigma_I)^{\wedge 2}$, skewness $Sk_I$, and kurtosis $(K_G)$.

$$Y1_{(aeolian:\ littoral)} = -3.5688M_Z + 3.7016\sigma_I^2 - 2.0766Sk_I + 3.1135K_G.$$

If Y1 is <-2.7411, the environment is littoral and if Y1 is >-2.7411, the environment is aeolian deposits.

$$Y2_{(beach:\ shallow\ agitated)} = 15.6534M_Z + 65.7091\sigma_I^2 + 18.1071Sk_I + 18.5043K_G.$$

If Y2 is <63.3650, shallow agitated water deposit (made up of larger grain sizes, because smaller grains have been washed out to deeper water) and if Y2 is >63.3650 indicates a beach deposit (an environment with different grain sizes where land, water, and air meet).

$$Y3_{(lacustrine:\ deltiac)} = 0.2852M_Z - 8.7604\sigma_I^2 - 4.8932Sk_I + 0.0482K_G.$$

If Y3 is <-7.4190, the environment is shallow lacustrine and if Y3 is >-7.4190 indicates deltaic deposition.

$$Y4_{(fluvial:\ turbidity)} = 0.7215M_Z - 0.4030\sigma_I^2 + 6.7322Sk_I + 5.2927K_G.$$

If Y4 is <9.8433, the fluvial deposition, and if Y4 is >9.8433 indicates turbidity current deposition.

The linear discriminate functions of core F3-08 (Y1, Y2, Y3, and Y4) according to units are present in Table 4 in their arithmetic average values.

Based on the Y1 values, all the studied samples fall in a littoral area and are affected by beach processes, except samples of unit V and a few samples from units I &II, which are plotted on the aeolian processes (Fig. 14A). The former group probably indicates that the core is located in an area close to the beach while the second group shows the periods of low lake levels corresponding to the arid climate and prevailing aeolian activity. Concerning the Y2 values, all samples fall in the beach environment (Fig. 14B). In addition, based on (Y3) most of the Holocene lacustrine sediments (units II-VI) are of shallow water lacustrine environment while those of late Pleistocene (unit I) are deposited under influence of the deltaic environment. With reference to the Y4 values, most of the Holocene lacustrine sediments are affected by a fluvial process while those of late Pleistocene (unit I) are deposited under the influence of the turbidity current environment (Fig. 14C).

The results of LDF cross-correlation indicate that the late Pleistocene Lake was much larger and deeper than the Holocene ones. Therefore, the fluvial processes are affected on the smaller and shallower Holocene Lake, and the larger and deeper late Pleistocene Lake are affected by turbidity current and deltaic environments.

**Table (4)** Average LDF values and C-M diagram of the six units of core F3-08

| Units | Depth (m) | LDF | | | | | | | | C-M | | | |
|---|---|---|---|---|---|---|---|---|---|---|---|---|---|
| | | Y1 | | Y2 | | Y3 | | Y4 | | C (One percentile in microns) | | M (Median in microns) | |
| VI | 0-3 | -9.54 | Aeolian | 322.2 | Beach deposition | -22.15 | Shallow lacustrine | 6.76 | Fluvial deposition | 388.41 | Suspension sediments | 6.39 | VIII |
| V | 3-4.7 | 3.1 | Aeolian | 506.8 | Beach deposition | -47.87 | Shallow lacustrine | 2.69 | Fluvial deposition | 1454.83 | Rolled sediments | 4.8 | IX |
| IV | 4.7-8.5 | -13.21 | Littoral | 275.51 | Beach deposition | -16.01 | Shallow lacustrine | 6.4 | Fluvial deposition | 320.34 | Suspension sediments | 5.25 | VIII |
| III | 8.5-10.3 | -14.35 | Littoral | 265.21 | Beach deposition | -13.26 | Shallow agitated marine | 5.83 | Fluvial deposition | 222.73 | Suspension sediments | 3.53 | VIII |
| II | 10.3-16.6 | -11.44 | Littoral | 295.47 | Beach deposition | -16.24 | Shallow lacustrine | 8.24 | Fluvial deposition | 389.39 | Suspension sediments | 3.67 | VIII |
| I | 16.6-22.7 | -9.93 | Littoral – Aeolian | 317.28 | Beach deposition | -15.05 | Deltaic | 17.68 | Turbidity current deposition | 1196.14 | Rolled sediments | 21.02 | III |

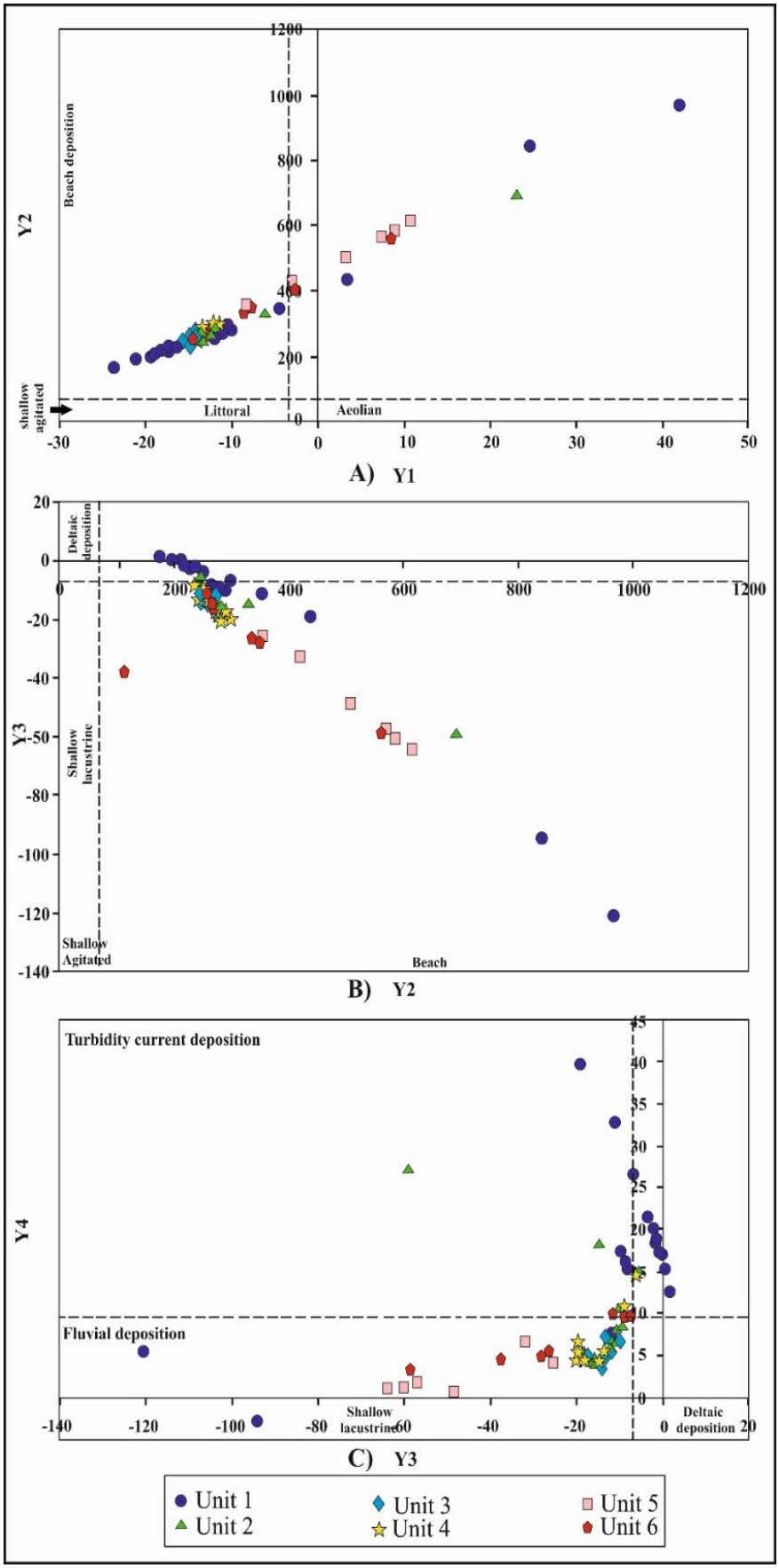


**Fig. (14)** Discrimination of environments of the core F3-08 units based on Linear Discrimination functions (LDF) plot, after (Sahu, 1964).

### 5.4. Mode of transportation (C-M diagram)

The C-M diagram has been used, after (Passega, 1964) to delineate the mode of transport along the core of F 3-08. The C-M diagram is based on the 1% percentage (one percentile) representing the maximum grain size and indicating the competency of the transporting agent, while the 50% percentage (fifty percentile) represents the median grain size of sediment transported. The C and M are presented in Microns, and their arithmetic average values according to each unit are given in Table 4.

The plotting points (Fig. 15) show clustering on the VIII field. Some points cluster on the III and IX fields. Unit I is denoted by C>1000 microns and M>15, 15<M>100, and M>200 microns of fields mainly VIII, IX, and I. This indicates mainly traction current transport where suspended sediments are incorporated. Unit II, III, and IV are denoted by C<1000 microns and M<15 microns and only three samples fall in the IX field. This indicates mainly suspension sediments where few rolled sediments were involved. Unit V is denoted by C>1000 microns and M>15 microns which indicates mainly rolled sediments. Unit VI is denoted by C<1000 microns and M<15 microns of the suspension sediments, only the top sample falls in the IX field indicating the rolled sediments of the flood plain. The clustering of plot values away from the C=M line indicates the poor sorting of the finer fraction. The slight vertical and horizontal change in C values causes transportation mechanism overlap that may be referred to varying grain size, and gravity of these grains, and influenced mainly by current and wave activity turbulence, in addition to the wind action influence.

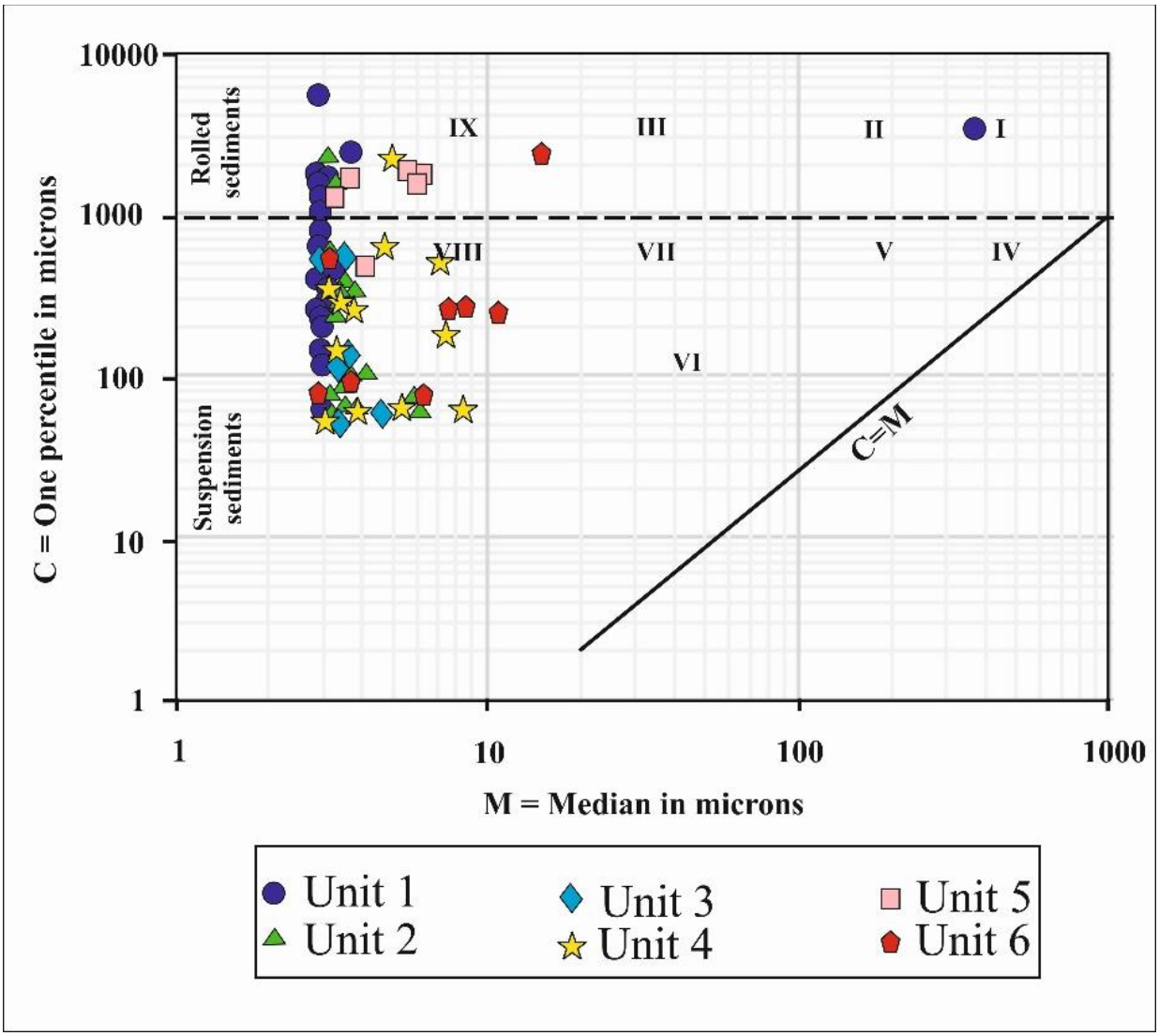


**Fig. (15)** C-M diagram showing the mode of transportation of core F3-08 units between C, (one percentile in Microns) and M (median size in microns) after (Passega, 1957, 1964; Passega and Byramjee, 1969).

**Conclusions**

The present study results conclude that the Faiyum paleolake sediments are heterogeneous. Depth controls the distribution of grain size (deeper is finer) with some sites that differ from this pattern. Sand fractions increased as the flood season started.

- Unit I (>10 cal. ka BP – late Pleistocene) is mainly clay with inter-fingering silty clay and coarse rounded quartz sand. It is considered the initial deep lake with reworked bedrock Eocene clay.
- Unit II (10-8 cal. ka BP - early Holocene) is composed of laminated silty clay with an abundance of ostracods, freshwater shells, and diatoms in varves representing seasonal lake.
- Unit III (8-6 cal. ka BP - early-middle Holocene) is massive silty clay with lots of carbonate concretions and fewer diatoms and shells indicating the Lacustrine delta front.
- Unit IV (6-4 cal. ka BP - late-middle Holocene) is clayey silt with iron oxide laminae and few white carbonate laminae and abundant carbonate and iron oxide concretion indicate lacustrine delta front.
- Unit V (4-2.4 cal. ka BP - late Holocene, Greece-Roman Recession) is sandy silty clay with some broken shells and rich in reworked fragments of pottery sherds representing a shallow lake.
- Unit VI (2.4 cal. ka BP- Recent - late Holocene, Ptolemaic times) is highly bioturbated sandy clayey silt with abundant Plant crusts indicating a floodplain environment.

Cumulative curves indicate that the suspension process of transport is dominant, as most sediments are fine sand or smaller. Frequency curves show a very wide range indicating the poorly to very poorly sorted nature of sediments. Distribution curves confirm that sediments are present in cycles of coursing upward along the core.

The sediments along the core are angular, coated, and dominated by poorly sorted, negative skewness values of coarse-skewed in nature indicating a low-energy environment. Except for the sandy part at the top of unit I, which has rounded, non-coated, moderately-sorted sediments with a positive skewness value of very fine skewed indicating the drought period and the aeolian input. Kurtosis values change along the core from very platykurtic to extremely leptokurtic indicating the circulation. Most mesokurtic nature qualified to the equal intermixing of the subordinate population with the predominant sediment mode and explained as a function of energy conditions sediments from riverine/aeolian processing.

The LDF analyses succeeded in delineating the process and environment of deposition. Accordingly, most of the Holocene sediments (units II, III, IV, V, and VI) of core F3-08 have a littoral nature, evident from their grain size distributions, deposited by fluvial current action, within the beach environment. The late Pleistocene sediments (Unit I) have a deltaic nature, deposited by turbidity current and also within the beach environment.

The C-M diagram succeeded in delineating the mode of the transport of sediments which is the tractive current of a river environment (Nile River) where the sediment mainly exhibits a graded suspension and suspension with rolling mode (saltation).

**References**

[1] Ashley, G. M. (1978). Interpretation of polymodal sediments. *The Journal of Geology*, *86*(4), 411-421.

[2] Baioumy, H. M., Kayanne, H., & Tada, R. (2010). Reconstruction of lake-level and climate changes in Lake Qarun, Egypt, during the last 7000 years. *Journal of Great Lakes Research*, *36*(2), 318-327.

[3] Ball, J. (1939). Contributions to the Geography of Egypt Survey. Cairo: Cairo Government Press.

[4] Bohacs, K. M., Carroll, A. R., Neal, J. E., Mankiewicz, P. J., Gierlowski-Kordesch, E. H., & Kelts, K. R. (2000). Lake-basin type, source potential, and hydrocarbon character: an integrated sequence-stratigraphic-geochemical framework. *Lake basins through space and time: AAPG Studies in Geology*, *46*, 3-34.

[5] Cloos, E., & Pettijohn, F. J. (1973). Southern Border of the Triassic Basin, West of York, Pennsylvania: Fault or Overlap? *Geological Society of America Bulletin*, *84*(2), 523-536.

[6] Flower, R. J., Stickley, C., Rose, N. L., Peglar, S., Fathi, A. A., & Appleby, P. G. (2006). Environmental changes at the desert margin: an assessment of recent paleolimnological records in Lake Qarun, Middle Egypt. *Journal of Paleolimnology*, *35*(1), 1-24.

[7] Flower, R. J., Keatings, K., Hamdan, M., Hassan, F. A., Boyle, J. F., Yamada, K., & Yasuda, Y. (2012). The structure and significance of early Holocene laminated lake sediments in the Faiyum depression (Egypt) with special reference to diatoms. *Diatom Research*, *27*(3), 127-140.

[8] Folk, R. L. (1955). Student operator error in determination of roundness, sphericity, and grain size. *Journal of Sedimentary Research*, *25*(4), 297-301.

[9] Folk, R. L., & Ward, W. C. (1957). Brazos River bar [Texas]; a study in the significance of grain size parameters. *Journal of sedimentary research*, *27*(1), 3-26.

[10] Folk, R. L. (1966). A review of grain- size parameters. *Sedimentology*, *6*(2), 73-93.

[11] Folk, R. L. (1974). The natural history of crystalline calcium carbonate; effect of magnesium content and salinity. *Journal of Sedimentary Research*, *44*(1), 40-53

[12] Friedman, G. M. (1967). Dynamic processes and statistical parameters compared for size frequency distribution of beach and river sands. *Journal of Sedimentary Research*, *37*(2), 327-354.

[13] Galehouse, J. S. (1969). Counting grain mounts; number percentage vs. number frequency. *Journal of Sedimentary Research*, *39*(2), 812-815.

[14] Garzanti, E., Andò, S., Padoan, M., Vezzoli, G., & El Kammar, A. (2015). The modern Nile sediment system: Processes and products. *Quaternary Science Reviews*, *130*, 9-56.

[15] Hamdan, M. A., Ibrahim, M. I. A., Shiha, M. A., Flower, R. J., Hassan, F. A., & Eltelet, S. A. M. (2016). An exploratory Early and Middle Holocene sedimentary record with palynoforms and diatoms from Faiyum Lake, Egypt. *Quaternary International*, *410*, 30-42.

[16] Hamdan, M. A., Flower, R. J., Hassan, F. A., & Hassan, S. M. (2020). The Holocene history of the Faiyum Lake (Egypt) based on sediment characteristics, diatoms and ostracods contents. *Journal of Great Lakes Research*, *46*(3), 456-475.

[17] Hamdan, M. A., & Hassan, F. A. (2020). Quaternary of Egypt. In *The geology of Egypt* (pp. 445-493). Springer, Cham.

[18] Hassan, F. A. (1986). Holocene lakes and prehistoric settlements of the Western Faiyum, Egypt. *Journal of Archaeological Science*, *13*(5), 483-501.

[19] Hassan, F. A., & Hamdan, M. A. (2008). The Faiyum Oasis-climate change and water management in ancient Egypt. *In Traditional Water Techniques: Cultural heritage for a sustainable future*. 6th Framework Programme, Shaduf Project, pp. 117-147.

[20] Hassan, F.A. Hamdan M.A, Flower, J. Tassie G. (2012a). Holocene geoarchaeology and water history of the Fayoum, Egypt. *In: Pirelli, R. (Ed.) Natural and Cultural Landscapes in the Fayoum.* The Safeguarding and Management of Archaeological Sites and Natural Environments. P. 116-133.

[21] Hassan, F.A., Hamdan, M.A., Flower, R. Keatings, K. (2012b). Oxygen and carbon isotopic records in Holocene freshwater mollusc shells from the Faiyumpalaeolakes, Egypt: palaeoenvironmental and palaeoclimatic implications. *Quaternary International* 266, 175-187.

[22] Hoelzmann, P., Gasse, F., Dupont, L. M., Salzmann, U., Staubwasser, M., Leuschner, D. C., & Sirocko, F. (2004). Palaeoenvironmental changes in the arid and sub arid belt (Sahara-Sahel-Arabian Peninsula) from 150 kyr to present. In *Past climate variability through Europe and Africa* (pp. 219-256). Springer, Dordrecht.Kasper-Zubillaga, J. J., & Carranza-Edwards, A. (2005). Grain size discrimination between sands of desert and coastal dunes from northwestern Mexico. *Revista mexicana de ciencias geológicas*, *22*(3), 383-390.

[23] Kasper-Zubillaga, J. J., & Carranza-Edwards, A. (2005). Grain size discrimination between sands of desert and coastal dunes from northwestern Mexico. *Revista mexicana de ciencias geológicas*, *22*(3), 383-390.

[24] Lane, A. (1938). III.—Medieval finds at Al Mina in North Syria. *Archaeologia*, *87*, 19-78.

[25] Little, O. H. (1936). Recent geological work in the Faiyum and adjoining portion of the Nile Valley. *Bulletin de L'Institut d 'Egypte*, 18, 201-240.

[26] Marks, L., Salem, A., Welc, F., Nitychoruk, J., Chen, Z., Blaauw, M., Zalat, A., Majecka, A., Szymanek, M., Chodyka, M., Tołoczko-Pasek, A., Sun, Q., Zhao, X. Jiang, J. (2018). Holocene lake sediments from the Faiyum Oasis in Egypt: a record of environmental and climate change. *Boreas*, 47, 62-79.

[27] Middleton, G. V. (1976). Hydraulic interpretation of sand size distributions. *The Journal of Geology*, *84*(4), 405-426.

[28] Milner, H.B. (1962). Sedimentary Petrography. Allen and Unwin, London, 207 pp.

[29] Moiola, R. J., & Weiser, D. A. N. I. E. L. (1968). Textural parameters; an evaluation. *Journal of Sedimentary Research*, *38*(1), 45-53.

[30] Passega, R. (1957). Texture as characteristic of clastic deposition. *AAPG Bulletin*, *41*(9), 1952-1984.

[31] Passega, R. (1964). Grain size representation by CM patterns as a geologic tool. *Journal of Sedimentary Research*, *34*(4), 830-847.

[32] Powers, M. C. (1953). A new roundness scale for sedimentary particles. *Journal of Sedimentary Research*, *23*(2), 117-119.

[33] Ray, A. K., Tripathy, S. C., Patra, S., & Sarma, V. V. (2006). Assessment of Godavari estuarine mangrove ecosystem through trace metal studies. *Environment International*, *32*(2), 219-223.

[34] Sahu, B. K. (1964). Depositional mechanisms from the size analysis of clastic

sediments. *Journal of Sedimentary Research*, *34*(1).

[35] Sawyer, D. E., Jacoby, R., Flemings, P., & Germaine, J. T. (2009). Data report: Particle size analysis of sediments in the Ursa Basin, IODP Expedition 308 Sites U1324 and U1322, northern Gulf of Mexico. *In Proc. IODP| Volume* (Vol. 308, p. 2).

[36] SLY, P. G. (1978). Sedimentary processes in lakes. In: *Lakes*. Springer, New York, NY. p. 65-89.

[37] Sutherland, R. A., & Lee, C. T. (1994). Discrimination between coastal subenvironments using textural characteristics. *Sedimentology*, *41*(6), 1133-1145.

[38] Visher, G. S. (1969). Grain size distributions and depositional processes. *Journal of Sedimentary Research*, *39*(3).

[39] Wendorf, F. Schild, R. (1976). Prehistory of the Nile Valley. *London: Academic Press.*